LASERLAB-EUROPE

The Integrated Initiative of European Laser Research Infrastructures III

Grant Agreement number: 284464

WP33
European Research Objectives on Lasers for Industry, Technology and Energy (EURO-LITE)

Deliverable number: 14

Feasibility study for the production of 1 at.%/2 cm diameter Yb:YAG ceramics

Lead Beneficiary:

National Institute for Laser, Plasma and Radiation Physics, Bucharest, Romania - INFLPR

Due date: 31.05.2014

Date of delivery: 09.05.2014

Project webpage: www.laserlab-europe.eu

Deliverable Nature	
R = Report, P = Prototype, D = Demonstrator, O = Other	R
Dissemination Level	
PU = Public PP = Restricted to other programme participants (incl. the Commission Services) RE = Restricted to a group specified by the consortium (incl. the Commission Services) CO = Confidential, only for members of the consortium (incl. the Commission Services)	PU

A. Abstract / Executive Summary

We report here on the work aimed at study the feasibility of producing Yb:YAG transparent ceramics with 1 at.% doping with typical centimeter scale size, starting from the powders selection and going through the material preparation. A brief account is given at the end of the experimental work of optical characterization of the obtained samples, as well as of the development of numerical tools to simulate the optical behavior of samples with a longitudinal doping gradient under thermal load, whose production feasibility study is expected to be carried out during the second part of activity.

B. Deliverable Report

1 Introduction

Ceramic materials deserve a growing attention as possible candidates to replace crystal materials as active medium in laser systems. Good mechanical properties, uniform composition, shorter production time, large slab size, superior micro-hardness and fracture toughness, together with higher doping level have been demonstrated. Nd:YAG and Yb:YAG ceramics have been successfully employed in high power lasers, with slab or disk geometry. Most importantly, ceramic materials present the further advantage of allowing an easy production of composite structures with different doping levels. These structured active media have been proposed as a possible solution to the need of a better thermal management. The final aim of the CNR activity (subcontracted from INFLPR) is the study of the feasibility of producing Yb:YAG ceramic laser media with low (1 at. %) doping and longitudinal doping gradient. Different CNR institutes are involved in this activity: ISTEC (Faenza) for the ceramics production, INO (Arcetri) and IFAC (Sesto Fiorentino) for the optical characterization of the samples and INO (Pisa and Arcetri) for the thermomechanical/optical simulations. In this first deliverable, we report in particular on the work aimed at demonstrating the feasibility of the production of Yb:YAG ceramics with 1 at.% doping and cm-scale size. After a detailed description of the production process, a brief account is given of the optical characterization of the samples. Finally, a preliminary discussion is given of the numerical simulation tools developed within EUROLITE.

2 Objectives

The first part of the EUROLITE project consists of a feasibility study for the production of Yb:YAG transparent ceramics with low doping level and medium diameter. This report summarizes the outcomes of the research work and the level achieved by the described approach.

3 Work performed / results / description

This deliverable describes the process used for the preparation of transparent Yb:YAG ceramics with 1 at.% Yb doping and the obtained results. The preparation route is solid state reaction sintering of oxide powders, which form the YAG phase *in-situ* and represents a favorable approach also for the preparation of structures with dopant gradient, which is the goal for the following deliverables.

POWDER SELECTION

A selection of starting materials (oxide powders) was made among commercially available powders (see Table 1) to identify the suitable ones. To achieve high transparency it is important that the powders are of high purity and possibly spherical shape with mean grain size in the nano- to submicrometric range. After a series of tests the following powders were selected: Al_2O_3 from Taimei, Y_2O_3 from Nanocerox and Yb_2O_3 from Alfa Aesar. The morphology of the selected powders is shown in Fig. 1.

Table 1. Properties of starting powders provided by producers.

Powder	Producer	S.S.A. m^2/g	D_{50} μm	Purity %	Phase RXD	Main impurities ppm
Al_2O_3	Taimei TM-DAR	17.22	0.20	>99.990	Al_2O_3	Si 3;Fe 7;Ca 2;Na,K, Mg 1
Al_2O_3	Baikalox CR30F	26	0.40	>99.990	Al_2O_3	Si 17;Fe 4;Na 7;Ca
Al_2O_3	Degussa Aeroxide AluC	100	0.013	>99.600	Al_2O_3	Fe 4; Na 7; Si 17; C 1
Y_2O_3	Treibacher	2.43	7.35	>99.999	Y_2O_3	SiO_2 20;Fe_2O_3 1; CaO 6; Al_2O_3 20; Na_2O 1; K_2O 2
Y_2O_3	Alfa Aesar	7.56	3.91	>99.999	Y_2O_3	Si 4;Fe 3;Na 2;Ca 1; K 1; Mg 1
Y_2O_3	China Rare Metals	23.32	0.03-0.05	>99.990	Y_2O_3	$Fe_2O_3$13; SiO_2 30; CaO 62; MgO 12
Y_2O_3	Starck	10-16	0.9	>99.95	Y_2O_3	-
Y_2O_3	Nanocerox	45.2	0.05	>99.99	Y_2O_3	Na 35; Al 7; Si 60; S 40; P 10; Cl 80; Ca 10; Fe 8
Y_2O_3	Pi-KEM	-	0.04	>99.99	Y_2O_3	-
Yb_2O_3	Sigma Aldrich	1.78	>1	>99.9	Yb_2O_3	Ca 21; Dy 6.1; Er 16
Yb_2O_3	Alfa Aesar	-	5.64	>99.99	Yb_2O_3	CaO 60; Fe_2O_3 3

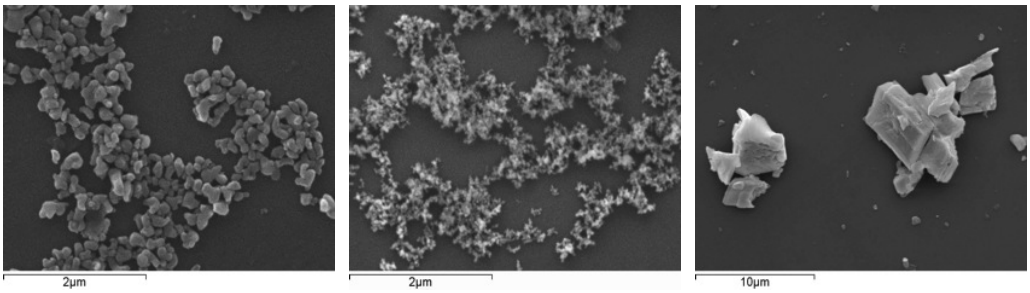

Fig. 1 SEM micrographs showing the morphology from left to right of Al_2O_3, Y_2O_3 and Yb_2O_3.

MATERIALS PREPARATION

Figure 2 illustrates schematically the material preparation process. A precise mixing and thorough homogenization of the oxide powders is crucial for obtaining transparent material with homogeneous dopant distribution and free of secondary phases. This is due to the high sensitivity of YAG ($Y_3Al_5O_{12}$) on stoichiometry, which has to be maintained carefully to avoid presence of alumina or another Y-Al-O phase (see Fig. 3).

The weight loss during heating was measured for all the powders, so that the stoichiometric ratio could be maintained with high precision. The weight loss is calculated from the difference between the weight of a pressed pellet before and after heating up to 1000 ℃. In order to avoid possible adsorption of humidity during cooling, the samples are moved to a desiccator at 200℃ and cooled to room temperature under vacuum before the second weighing. The weight loss values are particularly high in the case of very fine powders, which are reactive due to high specific surface area, and adsorb water when exposed to air.

The powders were mixed in stoichiometric ratio in absolute ethanol with the addition of organic dispersant (PEG 400) and TEOS. Tetraethyl orthosilicate (TEOS, 99.999%, Sigma-Aldrich, USA) was used as sintering additive in the amount of 0.5 wt.% with respect to the mass of solid. The mixture was homogenized by ball milling for 72 h in polyethylene bottles with 99.99% purity alumina balls, the powder : solvent : milling media weight ratio was 1:5:2.

This step is necessary for a good mixing of the oxides and the sintering additive, a crucial step for obtaining a homogeneous material. The homogenized suspension was spray dried by Mini Spray Dryer B-290 (Bu□chi Labortechnik AG, Switzerland). Spray drying is an advantageous technique for solvent removal, which has three interconnected features:

- Liquid phase removal while maintaining the homogeneity and enabling manipulation in the case of sub-micrometric and nanometric powders.
- Granulation of solid phase in spherical, monodispersed, fully dense granules, which can be easily formed by pressing.
- Quick and efficient recovering of the final material.

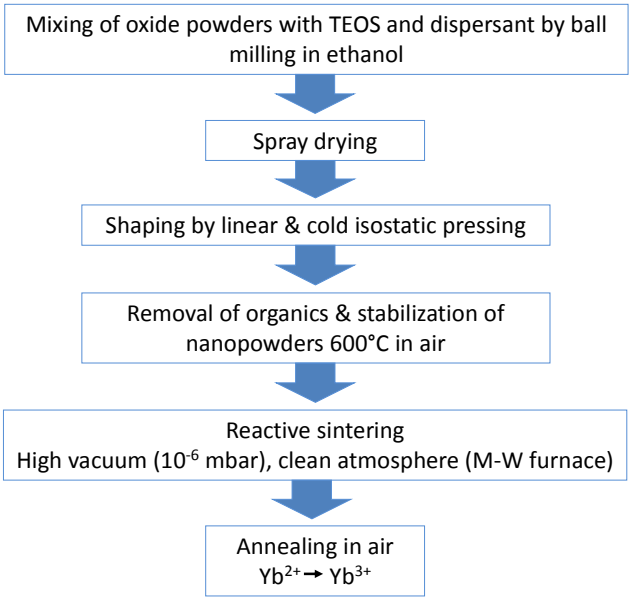

Fig. 2 Schematic description of the preparation process

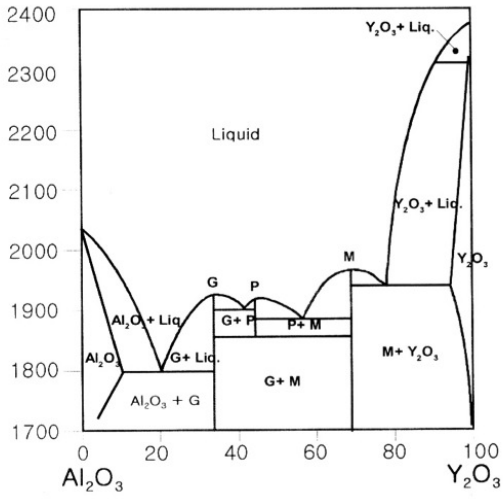

Fig. 3 Al_2O_3-Y_2O_3 phase diagram with YAG phase denoted as G.

The spray drying process is illustrated in Fig. 4: the suspension is sprayed through a heated nozzle by means of a drying medium (e.g. air or nitrogen). Due to the passage of the drying medium through the nozzle a sudden vaporization of the suspension occurs (Venturi effect), causing the formation of thousands of small droplets. The solvent evaporates and the ceramic powder within each droplet forms spherical solid aggregates.

The dried product separates from the drying medium in a cyclone under the effect of inertial forces and is recovered as down-going strain into a container at the base of the cyclone. The

size, shape and density of the spray dried aggregates can be manipulated by changing the spray drying parameters: temperature, flux and aspiration rate of the drying medium as well as solid content and feeding speed of the suspension. In order to obtain the desired granules, a balance must be found between the energy transported by the drying medium (determined by the medium temperature and flow), the energy transferred from the drying medium to the spray and the aspiration rate that defines the permanence time of the spray into the cyclone. The morphology of spray dried powders is illustrated in Fig. 5. The powder granules have spherical shape and size in the range from 1 to 10 μm, which was common for all the spray dried powders.

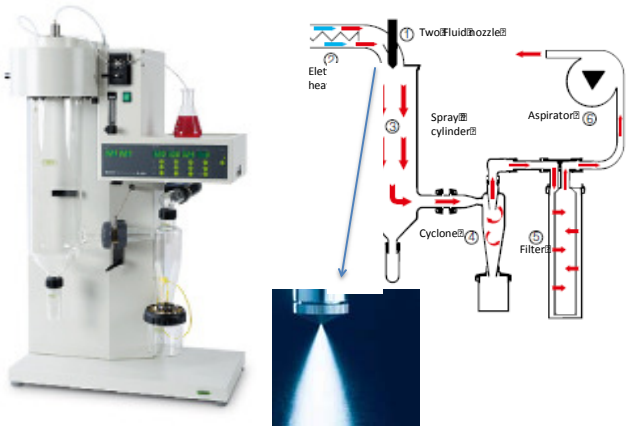

Fig. 4 Spray dryer; photograph and function scheme.

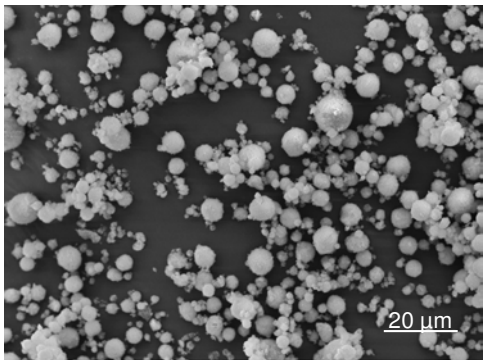

Fig. 5 Spray dried granules.

The spray dried powder was uniaxially pressed into pellets of in steel molds; here the sphericity of the granules helps to reach dense packing of particles during pressing. The formed samples are then cold isostatically pressed at 250 MPa. The density of pressed samples was about 54%-58% of the theoretical values.

Pressed samples were heat treated in air at 600℃ for one hour with the heating rate of 20℃/h in order to achieve full removal of any organic substances. A slow burnout process prevented any possible rapid gas evolution during burnout and thus helped in obtaining a homogeneous microstructure before the sintering step. The sintering (final material densification process) was performed in high vacuum (10^{-6} bar) at 1735℃ for 16 h in a clean furnace with chamber and heating elements made of molybdenum and tungsten. The applied vacuum represents an additional driving force that helps eliminate residual porosity from the microstructure. Annealing cycle was performed in air for 100 h at 1100℃. After the sintering in vacuum the materials contain oxygen vacancies, which lead to light scattering, and the Yb^{3+} ions are reduced to Yb^{2+}, which gives the material green coloration (see Fig. 6). The applied annealing cycle allowed the reoxidization of Yb^{2+} to the laser active Yb^{3+} and the removal of oxygen vacancies without further grain growth or segregation of secondary phases, which has been observed after annealing at higher temperatures.

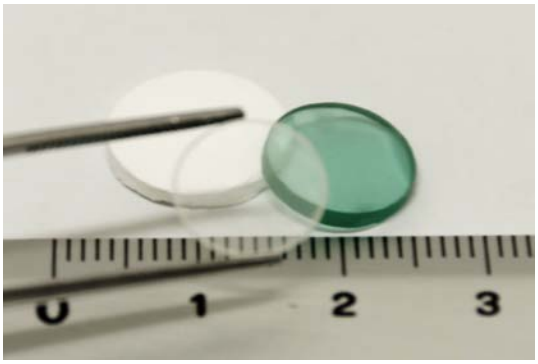

Fig. 6 Pressed (white opaque), as-sintered (green) and sintered sample after annealing (colorless).

CHARACTERIZATION

The sintered samples were polished with diamond pastes and sprays down to 0.25 μm, their densities were measured via the Archimedes' method, and microstructure was observed with electron microscope. The optical quality of polished annealed samples was characterized via transmittance measurements on UV/Vis spectrophotometer (Lambda 35 UV/Vis, PerkinElmer, USA). X ray diffraction analysis was used for monitoring of the evolution of phases during sintering for controlling the final composition.

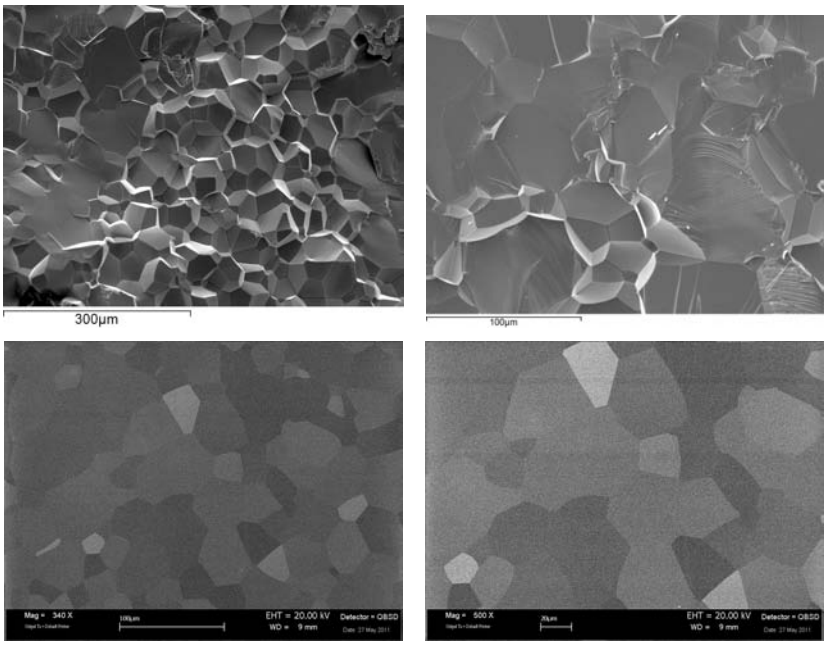

Fig. 7 SEM micrographs of the sintered samples; fractured surface and surface after polishing showing the grain size.

The sintered samples had homogeneous microstructure (see Fig. 7), with almost no residual porosity. The measurements by the Archimedes' method confirmed that the samples were sintered to full density and from the X ray diffraction results the only phase in the material is YAG. Mean grain size is about 30 μm.

For the purpose of optimization of the preparation process, also YAG without dopant was prepared, as well as samples with higher Yb content. From the results we can say that Yb does not support sintering of YAG, and higher additions required for example higher sintering temperatures. The difference between dopant-free and 1 at.% Yb:YAG was not significant, and the same sintering cycle can be used with good results (see optical transmittance of the sintered samples in Fig. 8). However, it was observed that larger samples did not sinter to the same quality under the same conditions as smaller ones, and a certain amount of

residual porosity remained in the central part of the material. After an evaluation of preparation process, modifications were implemented, which helped resolve this complication. Apparently, for larger pieces, longer sintering times are required to allow the diffusion of residual gas from the inner part of the material and the closure of pores. Figure 9 shows sintered samples of different diameter and thickness.

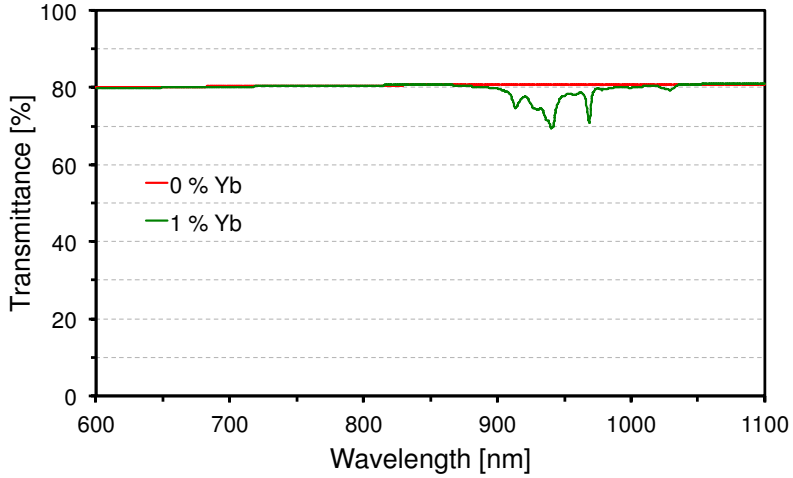

Fig. 8 Transmittance spectra of samples sintered at 1735°C for 16 h; measured by 35 UV/Vis, Perkin Elmer spectrophotometer.

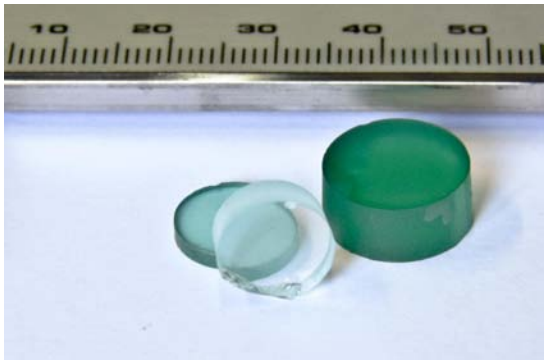

Fig. 9 Sintered 1 at.% Yb:YAG samples of different sizes.

LASER PERFORMANCES

Preliminary laser characterization was performed in a V-shaped laser cavity as shown in Fig. 10. The active sample is optically pumped through the dichroic (high transmission at 940 nm and high reflectivity at the laser wavelength, i.e. 1030 nm) flat end mirror. The cavity is folded by about 10° by a highly reflective mirror with a radius of curvature of 150 mm. The cavity is completed by a flat output coupler mirror that has been used with various transmission values (TOC) between 1.5% and 20%. The sample is brazed by Indium to a water cooled heat sink. The optical pumping of the sample is done with a diode laser with nominal emission wavelength of 940 nm coupled to a fiber with a 200 micron core diameter and a NA of 0.22. The excitation beam is focused on the sample by means of two achromatic doublets with a nominal unit magnification ratio resulting in a waist radius of 130 micron at 1/e2. The cavity arrangement is set to obtain a cavity mode inside the active medium smaller with respect to the pump mode in order to get a uniform pump in the cavity mode volume. The proximity of the sample to the end mirror reduces the influence of thermal lensing on the cavity stability. in order to reduce the thermal lensing the pump diode is operated with a square wave modulation at 10 Hz and 20% duty factor.

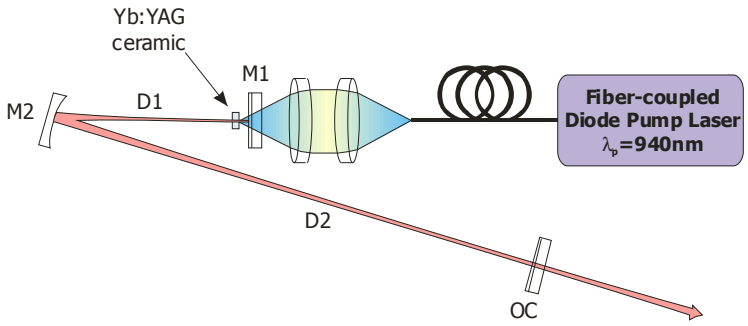

Fig. 10 Set up for laser characterization; D1= 85 mm, D2= 240 mm.

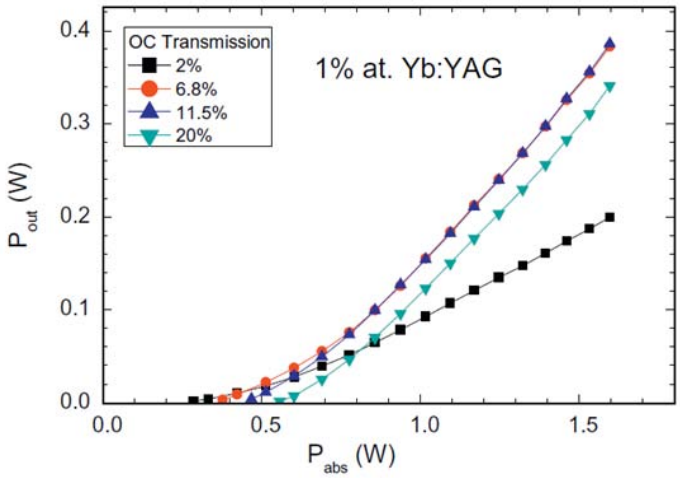

Fig. 11 Laser output power as a function of the absorbed output power, for several values of the output coupler transmission.

The tested sample (thickness 1.25 mm) showed a maximum slope efficiency of 39.5% with T_{OC}= 6.8%, with a P_{max} of 0.39 W (see Fig. 11).

NUMERICAL SIMULATIONS

In view of the optimization of the longitudinal doping gradient structure, a numerical simulation code was developed, aimed at studying the wavefront aberrations induced in high repetition rate amplifiers. The code is able to calculate the transverse wavefront profile of a laser pulse after the propagation through a laser amplifier. The code takes into account the thermomechanical properties of the active medium and takes as input the thermal load induced by the pump absorption and the subsequent nonradiative relaxation. As an example, Fig. 12 *left)* shows a sketch of a simulated active medium mount and Fig. 12 *right)* shows the temperature distribution for different longitudinal doping gradient structure. Further details and results will be given in the final deliverable report.

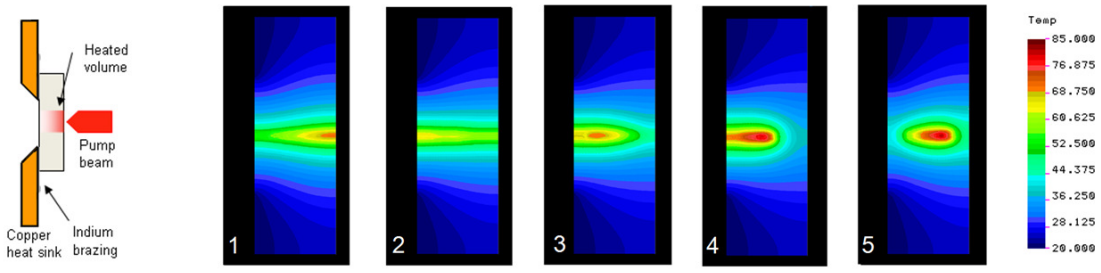

Fig. 12 *left)* Sketch of an active medium mount geometry simulated; *right)* temperature distribution map as obtained for Yb:YAG slabs with different longitudinal doping gradient.

4 Conclusions & Summary

Transparent 1 at. % Yb:YAG ceramics were prepared at CNR ISTEC. Suitable starting materials were selected and the preparation process was analyzed with respect to the dimension scaling and to the presence of dopant. The production process leads to transparent ceramics without secondary phases and with minimum residual porosity, both of which are crucial factors affecting the optical and laser quality of the material. Samples with transmittance above 80% have been prepared and a preliminary laser performance test was carried out with positive outcomes. In addition, it has to be said that another preparation method was identified for the production of materials with larger diameter: the tape casting. This method is based on the preparation of thin sheets with high organic content, which can be stacked and pressed into bulk samples. This approach is especially interesting for further introduction of dopant gradient and will be further tested for the following deliverables.

At the same time, a numerical tool was developed for the simulation of the wavefront distortions induced by the pumping process in ceramic laser media with longitudinal doping gradients, whose feasibility study is envisaged as the next activity within EUROLITE.

The financing from the LaserLab-Europe, EuroLite project was acknowledged in two publications, one paper that was published in a SPIE proceeding and an article that was published in the Opt. Express journal.

5a. References

M. Mizuno and T. Noguchi, Rep. Govt. Ind. Res. Inst. Nagoya, 16, 171 (1967).
L. Esposito, A. Piancastelli, “Role of powder properties and shaping techniques on the formation of pore-free YAG materials,” J. Eur. Ceram. Soc. **29**, 317 (2009).
D. Alderighi, A. Pirri, G. Toci, M. Vannini, L. Esposito, A. L. Costa, A. Piancastelli, M. Serantoni, “Characterization of Yb:YAG ceramics as laser media,” Opt. Mat. **33**, 205-210 (2010).
L. Esposito, A. Piancastelli, A. L. Costa, M. Serantoni, G. Toci, M. Vannini, “Experimental features affecting the transparency of YAG ceramics,” Opt. Mat. **33**, 346–354 (2011).

5b. Publications

1. A. Lapucci, M. Ciofini, L. Esposito, P. Ferrara, L.A. Gizzi, J. Hostasa, L. Labate, A. Pirri, G. Toci, M. Vannini, “Characterization of Yn:YAG active slab media based on a layered structure with different doping,” Proc. SPIE **8780**, 87800J1 (2013).
http://spie.org/Publications/Proceedings/Volume/8780?origin_id=x4318&event_id=1022237

2. P. Ferrara, M. Ciofini, L. Esposito, J. Hostasa, L. Labate, A. Lapucci, A. Pirri, G. Toci, M. Vannini, L.A. Gizzi, “3D numerical simulation of Yb:YAG active slabs with longitudinal doping gradient for thermal load effects assessment,” Opt. Express **22** (5), 5375 (2014).
DOI:10.1364/OE.22.005375
http://www.opticsinfobase.org/oe/abstract.cfm?URI=oe-22-5-5375&origin=search